minerals

MDPI

Article

Microstructural Constraints on Syn- to Post-Magmatic Deformation of North Bangka Granitoids, Indonesian Segment of the Southeast Asian Tin Belt

Muhammad Iqbal Septiandi [1], Mirzam Abdurrachman [1,2,*], Nurcahyo Indro Basuki [1], Emmy Suparka [3], I Gusti Bagus Eddy Sucipta [1], Prihadi Sumintadireja [1], Moh Fadhly Rizki Yazid [4] and Muhammad Bahrun Najah [5]

[1] Department of Geological Engineering, Institut Teknologi Bandung (ITB), Jalan Ganesha No. 10, Bandung 40132, Indonesia; 22023307@mahasiswa.itb.ac.id (M.I.S.); n.basuki@itb.ac.id (N.I.B.); sucipta@itb.ac.id (I.G.B.E.S.); prihadi@itb.ac.id (P.S.)
[2] Graduate School of Multidisciplinary Science and Technology, Institut Teknologi Bandung (ITB), Jalan Ganesha No. 10, Bandung 40132, Indonesia
[3] Department of Geological Engineering, University of Pertamina, Jakarta 12220, Indonesia; made.er@universitaspertamina.ac.id
[4] School of Environment, University of Auckland, Private Bag 92019, Auckland 1142, New Zealand; myaz495@aucklanduni.ac.nz
[5] Department of Geosciences, University of Padova, Via VIII Febbraio, 2, 35122 Padova, Italy; muhammadbahrun.najah@studenti.unipd.it
* Correspondence: mirzam@itb.ac.id

Abstract

Granitoids in North Bangka, Bangka Belitung Province, Indonesia, are an integral part of the Southeast Asian Tin Belt magmatism, yet their deformation history from crystallization through tectonic cooling remains incompletely documented. This study characterizes the petrography and reconstructs the microstructural deformation history of granitoids. Nine representative granitoid samples were collected from outcrops at Bukit Bias, Tempilang, Siangau, Mangkol, Kelapa, Jebus, Pemali, Plangas, and Menumbing (Nikon Eclipse LV100NPOL (Nikon Corporation, Tokyo, Japan) with NIS-Elements BR software, Basic Research Version) and modal point counting (3608 points per section) were applied to ensure a more detailed description and accurate quantification of mineral compositions. The granitoids are classified as syenogranite, monzogranite, and quartz syenite based on the QAP modal diagram. The dominant minerals are K-feldspar (24.89–54.27 vol.%), quartz (16.47–37.13 vol.%), and plagioclase (10.89–24.45 vol.%), with biotite as the femic phase. Microstructural analysis reveals three successive deformation stages: (1) a suprasolidus stage (T > 650 °C) marked by submagmatic fractures, grain boundary migration (GBM) in feldspar and chessboard pattern quartz; (2) a high-temperature subsolidus stage (650–450 °C) characterized by GBM and subgrain rotation recrystallization in quartz, myrmekite, and flame perthite; and (3) a low-temperature subsolidus stage (T < 450 °C) evidenced by undulose extinction, bulging recrystallization (BLG), deformation twins in feldspar, and kink bands in feldspar and mica. The progressive microstructural sequence demonstrates that deformation was initiated during the late magmatic stage and persisted under decreasing temperature in the solid state, indicating that the North Bangka granitoids record a prolonged history of syn- to post-magmatic deformation linked to the regional tectono-magmatic evolution of the Southeast Asian Tin Belt. These granitoids belong to the Late Triassic–Early Jurassic (228–198 Ma) Klabat Granite Complex, emplaced within the Indonesian segment of the belt during the Sibumasu–Indochina collision, and the microstructural evolution documented here is consistent with this regional tectono-magmatic history.

Check for updates

Academic Editor: Chad D. Deering

Received: 21 June 2026
Revised: 23 July 2026
Accepted: 27 July 2026
Published: 29 July 2026

Copyright: © 2026 by the authors. Licensee MDPI, Basel, Switzerland. This article is an open access article distributed under the terms and conditions of the Creative Commons Attribution (CC BY) license.

Keywords: granitoid; petrography; microstructure; deformation; Southeast Asian Tin Belt; Bangka; recrystallization; tectonic

1. Introduction

The Southeast Asian Tin Belt (SATB) represents one of the most significant metallogenic provinces in the world, extending from Myanmar through Thailand, Peninsular Malaysia, and into the Indonesian islands of Bangka and Belitung [1,2]. Granitic plutonism played a fundamental role in the genesis of tin mineralization across this belt, and the Bangka archipelago constitutes its southernmost exposed segment [3,4].

North Bangka is dominated by the Klabat Granite, a Late Triassic to Early Jurassic intrusive complex [5], emplaced into an older metasedimentary basement (Pemali Complex) and coeval mafic intrusions (Penyabung Diabase). The regional structural fabric trends NNW–SSE and NNE–SSW, reflecting a kinematic history linked to the Sibumasu–Indochina collision and oblique Sunda Shelf subduction [6,7]. Although the geochemical affinity of Bangka granitoids has been established by previous workers [8], the textural and microstructural record of syn- to post-magmatic deformation has not been systematically documented.

Granitic textures and microstructures encode successive deformation stages from near-solidus magmatic conditions through solid-state deformation at progressively lower temperatures [9,10]. The identification of diagnostic microstructures—such as submagmatic fractures, grain boundary migration (GBM), subgrain rotation (SGR), bulging recrystallization (BLG), myrmekite, flame perthite, deformation twins, and kink bands—enables the reconstruction of a temperature deformation path calibrated against experimentally constrained thermometers [11–13].

These temperature assignments are grounded in well-established experimental and natural calibration studies. Quartz recrystallization regimes follow the experimentally defined sequence of bulging recrystallization (BLG; <400 °C), subgrain rotation (SGR; 400–500 °C), and grain boundary migration (GBM; >500 °C) [12]. Feldspar-related microstructures are interpreted according to established frameworks [11,13], while myrmekite and flame perthite are evaluated using the criteria of [13,14]. Although individual temperature estimates carry semi-quantitative uncertainties (typically ±50 °C), the consistency across multiple, independently calibrated indicators (quartz fabrics, feldspar recrystallization, and deformation-induced reaction textures) significantly strengthens the reliability of the overall temperature–deformation path reconstructed in this study.

Despite these methodological advances, the timing and tectonic significance of deformation during granite emplacement and cooling remain poorly constrained in the Indonesian segment of the Southeast Asian Tin Belt (SATB). It is still unclear whether deformation was primarily syn-magmatic (related to active tectonism during pluton emplacement) or developed later as post-magmatic tectonic reactivation. Resolving this issue is critical because deformation microstructures can record the tectonic conditions responsible for granite emplacement and subsequent crustal evolution across the SATB.

North Bangka granitoids provide an excellent opportunity to address this problem because they represent part of the Klabat Granite Complex, one of the major granitoid bodies in the Indonesian sector of the SATB. Although previous studies have established their Late Triassic age and regional tectonic affinity, little attention has been paid to the microstructural evidence that records deformation during and after magma crystallization. Consequently, the relationship between granitoid emplacement, cooling history, and regional tectonic processes remains poorly understood.

The present study aims to do the following: (1) characterize the modal mineralogy and rock classification of North Bangka granitoids through systematic point counting; (2) document the succession of deformation microstructures across the three lithological types identified; and (3) reconstruct the microstructural evolution and its implications for the regional tectonic history of the SATB.

Although previous studies have established the regional distribution, age, and geochemical affinity of Bangka granitoids, the microstructural record of their emplacement, cooling, and post-crystallization deformation remains poorly constrained. This gap limits our ability to evaluate whether the granitoids record purely magmatic crystallization, syn-magmatic deformation, or later solid-state reworking.

2. Geological Setting

The study area encompasses the northern part of Bangka Island (Figure 1), bounded by coordinates 105°06′30.41″ E–106°13′42.35″ E and 01°30′04.05″ S–02°18′41.27″ S, within Bangka Regency and West Bangka Regency, Bangka Belitung Islands Province, Indonesia.

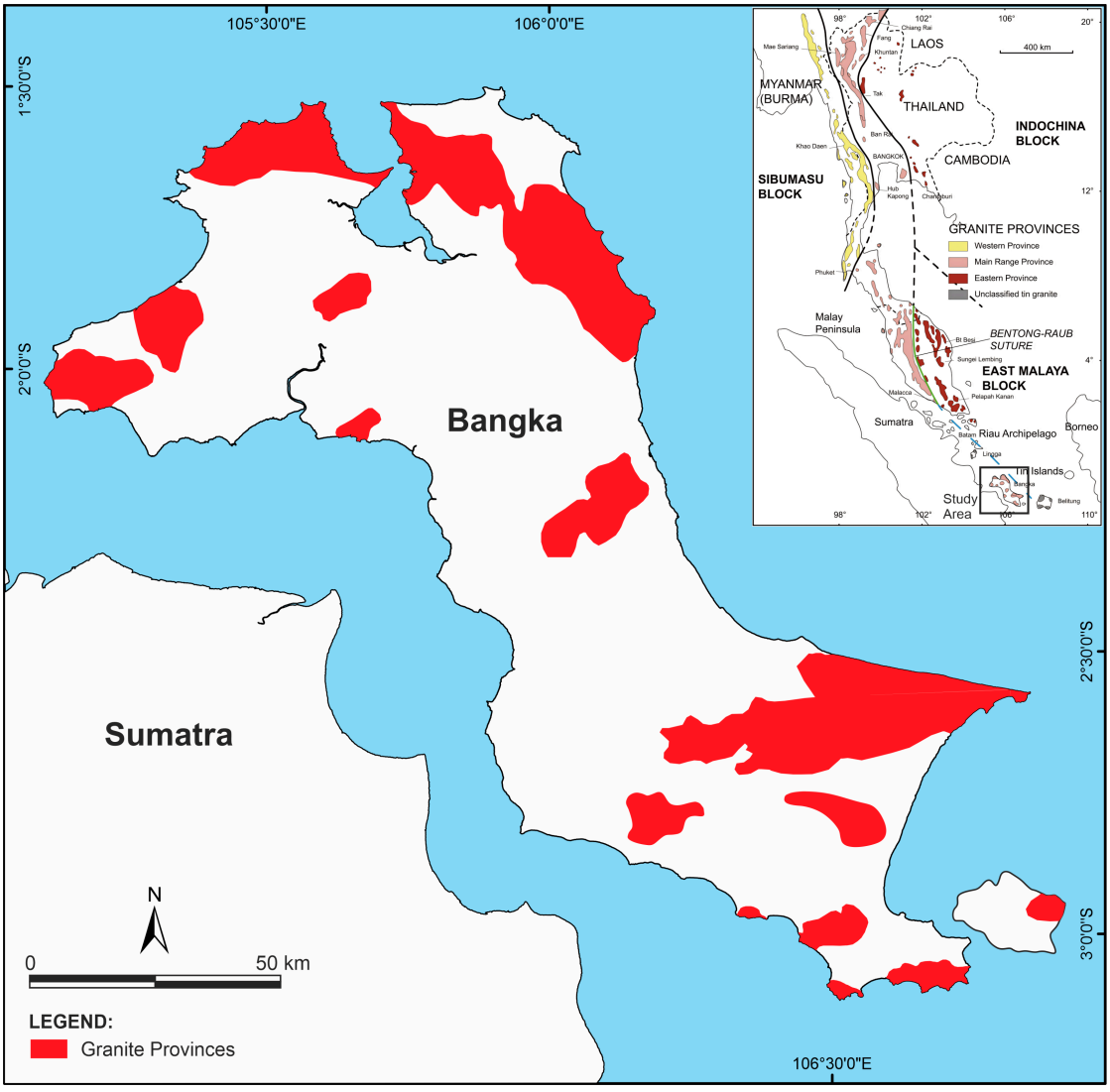


Figure 1. Spatial distribution of granite provinces on Bangka Island, Indonesia, with granite-bearing areas shown in red (modified after [8]). The inset illustrates the Southeast Asian Tin Belt and its three granite provinces as defined by [1].

The stratigraphy of North Bangka consists of the following, from oldest to youngest: the Pemali Complex (low-grade metasediments), the Penyabung Diabase (coeval mafic intrusions), the Tanjunggenting Formation (clastic sediments), the Klabat Granite (Late Triassic–Early Jurassic, 228–198 Ma [8]), the Ranggam Formation (Neogene sediments), and Quaternary alluvial deposits [5]. The Klabat Granite constitutes the principal plutonic unit in the study area (Figure 2). The timing of granitoid magmatism in North Bangka is further constrained by published Sm–Nd isotopic data from [8]. These data indicate Late Triassic ages for several granitoid bodies, including Belinyu quartz syenite at 227 Ma, Pelangsa monzogranite at 223 Ma, Pemali syenogranite at 222 Ma, and Menumbing syenogranite at 219 Ma. The narrow age range of 227–219 Ma suggests that the studied granitoids formed during a relatively restricted magmatic episode, directly related to regional tectono-magmatic activity associated with the Southeast Asian Tin Belt.

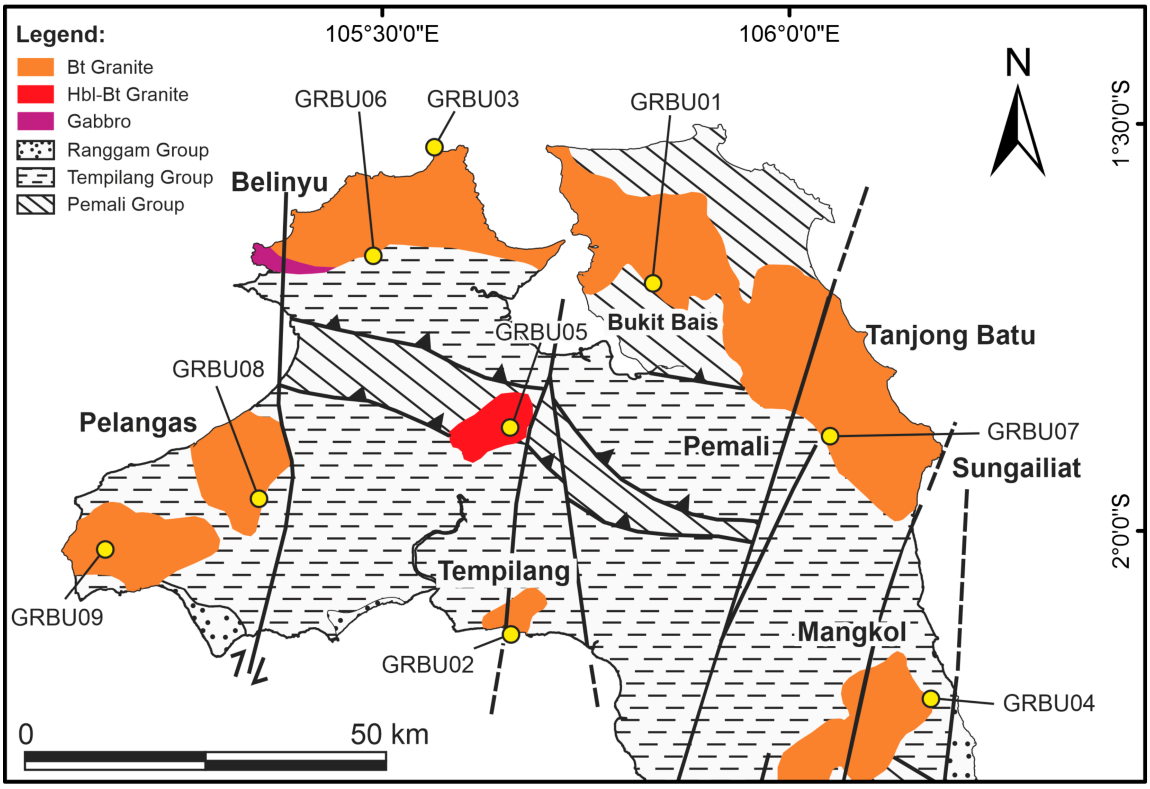


Figure 2. Geological map of the study area and distribution of granitoid samples (modified from [8]). Sample codes GRBU01–GRBU09 mark collection localities.

The regional architecture is controlled by two dominant fault sets trending NNW–SSE and NNE–SSW, interpreted as products of the Sibumasu–Indochina continental collision during the Middle to Late Triassic and subsequently reactivated during oblique subduction along the Sunda margin [6,7]. These structures exerted a first-order control on the emplacement geometry and post-emplacement deformation of the Klabat Granite. Consequently, the North Bangka granitoids provide an excellent opportunity to investigate the microstructural record of syn- to post-magmatic deformation within a well-constrained tectonic framework, allowing reconstruction of the temperature-deformation path from near-solidus conditions to lower-temperature solid-state deformation.

3. Materials and Methods

3.1. Sample Collection

Nine samples were collected from representative outcrops distributed across North Bangka (Table 1). Sample codes GRBU01 through GRBU09 correspond to localities at Bukit Bias, Tempilang, Siangau, Mangkol, Kelapa, Jebus, Pemali, Plangas, and Menumbing, respectively. These granitoid samples were chosen to represent the spatial variability of rock types and deformation intensity across the study area. Standard polished thin sections (30 μm thickness) were prepared for each sample.

Table 1. Sample localities and UTM Zone 48S (WGS 84) coordinates of granitoid samples from North Bangka.

Sample Code	Locality	District	Easting (m)	Northing (m)
GRBU01	Bukit Bias	Bangka	592,657.42	9,812,554.75
GRBU02	Tempilang	West Bangka	573,484.00	9,764,898.49
GRBU03	Siangau	Bangka	562,780.37	9,830,989.36
GRBU04	Mangkol	Bangka	630,515.93	9,756,146.84
GRBU05	Kelapa	West Bangka	574,345.80	9,789,872.24
GRBU06	Jebus	West Bangka	554,501.82	9,816,301.75
GRBU07	Pemali	Bangka	616,790.68	9,791,813.70
GRBU08	Plangas	West Bangka	541,103.99	9,784,498.33
GRBU09	Menumbing	West Bangka	517,945.60	9,776,480.68

Coordinates are in UTM Zone 48S, WGS 84 datum.

3.2. Petrographic Analysis

Petrographic analysis was performed at the Petrography Laboratory, Department of Geothermal Engineering, Institut Teknologi Bandung, Indonesia, using a Nikon Eclipse LV100NPOL polarized-light microscope equipped with NIS-Elements Basic Research imaging software. For each thin section, full-plate photomosaics were acquired under plane-polarized light (PPL) and cross-polarized light (XPL). Modal mineral proportions were quantified through systematic grid-based point counting, with 3608 points counted per thin section. Mineral phases were identified based on standard optical properties used in igneous and metamorphic petrography [14].

3.3. Rock Classification

Rock names were assigned using the QAPF (QAP) modal classification diagram of [15], with Qz (quartz), A (alkali feldspar), and P (plagioclase) recalculated to 100%. Modal data were plotted on a QAP diagram to identify the rock types present.

3.4. Microstructural Analysis

Microstructural analysis was conducted to identify deformation mechanisms and to infer the relative temperature conditions under which they developed. Because no direct thermometric measurements were performed in this study, the temperature estimates are treated as qualitative to semi-quantitative constraints derived from published microstructural criteria. The interpretation follows established thermometric frameworks [11,13] together with the quartz recrystallization regime [12], which distinguishes bulging recrystallization (BLG; <400 °C), subgrain rotation recrystallization (SGR; 400–500 °C), and grain boundary migration recrystallization (GBM; >500 °C). Feldspar-related microstructures were interpreted using Pryer and Robin [16] for flame perthite and Paterson et al. [17]

for magmatic versus solid-state deformation criteria. The temperature ranges adopted here are therefore treated as relative, literature-calibrated indicators rather than precise thermometric determinations. This approach follows standard practice in microstructural studies of granitoids [11–13] and is justified by the convergence of multiple independent microstructural criteria.

4. Results

4.1. Rock Classification and Modal Mineralogy

Based on QAP modal classification, the North Bangka granitoids are dominated by syenogranite (GRBU01, GRBU02, GRBU04, GRBU06, GRBU07, GRBU09), with subordinate monzogranite (GRBU05, GRBU08) and one sample of quartz syenite (GRBU03) (Figure 3; Table 2). Photomicrographs of representative thin sections are shown in Figure 4.

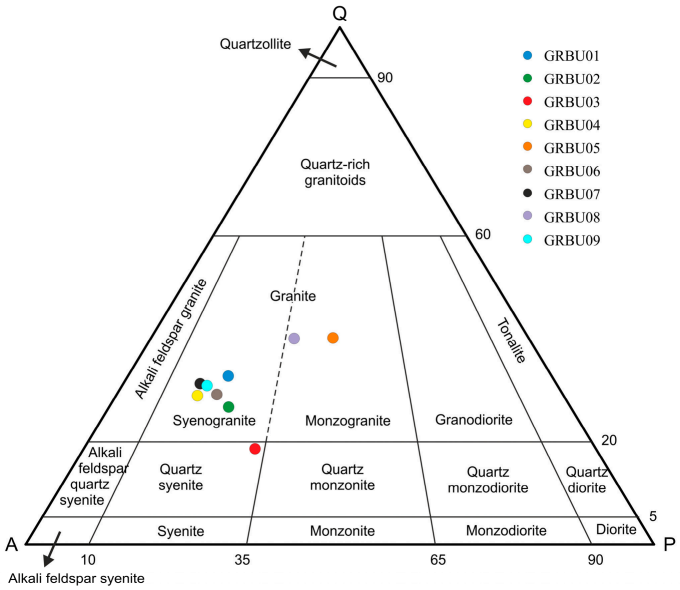


Figure 3. QAP modal classification diagram showing the compositional range of North Bangka granitoids [15].

Table 2. Textural characteristics of North Bangka granitoid samples.

Sample	Locality	Rock Name	Texture	Crystal Size (mm)
GRBU01	Bukit Bais	Syenogranite	Equigranular hypidiomorphic	<0.1–5
GRBU02	Tempilang	Syenogranite	Equigranular hypidiomorphic	<0.1–7
GRBU03	Siangau	Quartz Syenite	Inequigranular porphyritic	<0.1–9
GRBU04	Mangkol	Syenogranite	Equigranular hypidiomorphic	<0.1–8
GRBU05	Kelapa	Monzogranite	Equigranular hypidiomorphic	<0.1–7
GRBU06	Jebus	Syenogranite	Equigranular hypidiomorphic	<0.1–9
GRBU07	Pemali	Syenogranite	Inequigranular porphyritic	<0.1–11
GRBU08	Plangas	Monzogranite	Inequigranular porphyritic	<0.1–14
GRBU09	Menumbing	Syenogranite	Inequigranular porphyritic	<0.1–10

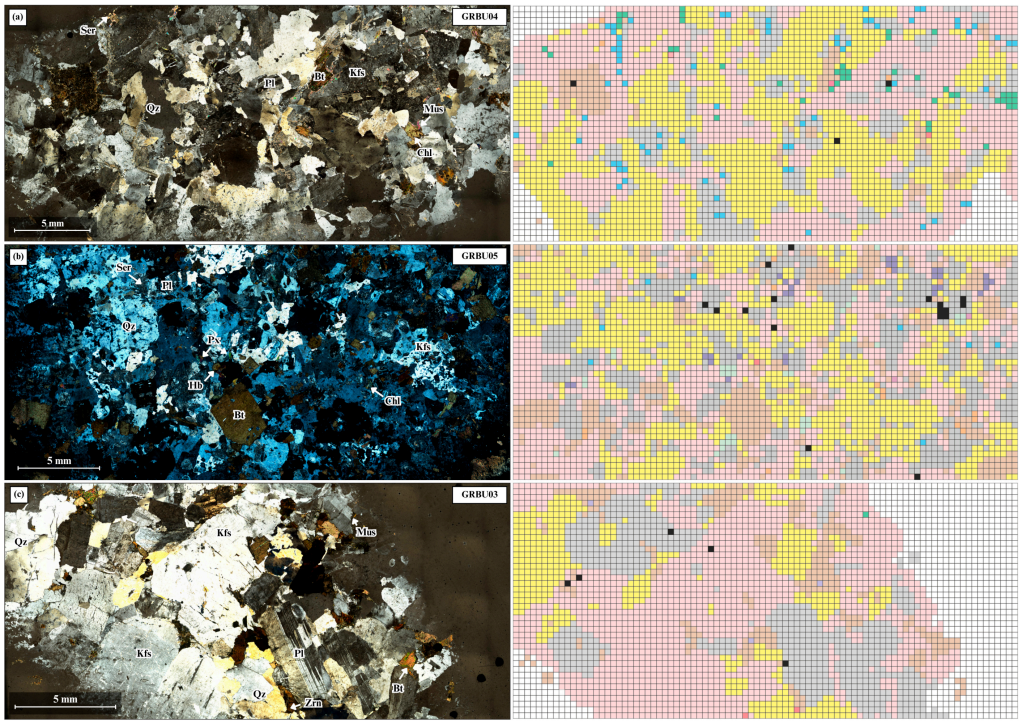


Figure 4. Representative photomicrographs of North Bangka granitoids under cross-polarized light (XPL), accompanied by point-counting modal analysis results for each sample. (**a**) Syenogranite (GRBU04) showing equigranular hypidiomorphic texture; (**b**) point-counting map for GRBU04; (**c**) monzogranite (GRBU05) with balanced feldspar proportions; quartz syenite (GRBU03) showing inequigranular texture. Mineral abbreviations: Qz = Quartz; Kfs = K-Feldspar; Pl = Plagioclase; Bt = Biotite; Ms = Muscovite; Hb = Hornblende; Px = Pyroxene; Opq = Opaque Mineral; Zrn = Zircon; Ser = Sericite; Chl = Chlorite. The colors used in the point-counting maps indicate the following mineral phases: yellow = quartz; pink = K-feldspar; grey = plagioclase; brown = biotite; green = muscovite; pale green, = hornblende; dark blue = pyroxene; black = opaque mineral; red = zircon; purple = apatite; light blue = sericite; and orange = chlorite.

All samples exhibit granitic to quartz-syenitic modal compositions and display a range of textures from equigranular hypidiomorphic to inequigranular porphyritic (Table 2). Crystal sizes vary from less than 0.1 mm to a maximum of 14 mm, with the largest phenocrysts observed in the porphyritic samples (GRBU07, GRBU08, and GRBU09). K-feldspar is the dominant mineral in most samples, ranging from 24.89 vol.% (GRBU05) to 54.27 vol.% (GRBU07). Quartz content ranges from 16.47 vol.% (GRBU03) to 37.13 vol.% (GRBU08). Plagioclase varies from 10.89 vol.% (GRBU07) to 24.45 vol.% (GRBU05). Biotite is the principal mafic mineral (0.78–14.27 vol.%), with hornblende and pyroxene restricted to sample GRBU05 (Table 3). Accessory minerals include zircon, apatite, and tourmaline (GRBU08). Secondary minerals (sericite, chlorite) are present in variable amounts, indicating low-grade hydrothermal alteration.

4.2. Deformation Microstructures

Microstructural analysis reveals a consistent progression of deformation features across all three lithological types (syenogranite, monzogranite, and quartz syenite). Three stages of deformation are recognized, from high- to low-temperature conditions (Figures 5–7).

Table 3. Modal mineral composition (vol.%) of North Bangka granitoids from point counting (3608 points per section). Mineral abbreviations are after [18]. Qz = quartz; Kfs = K-feldspar; Pl = plagioclase; Bt = biotite; Hb = hornblende; Ms = muscovite; Opq = opaque; Px = pyroxene; Zrn = zircon; Ap = apatite; Tur = tourmaline; Ser = sericite; Chl = chlorite.

Sample	Qz	Kfs	Pl	Bt	Hb	Ms	Opq	Px	Zrn	Ap	Tur	Ser	Chl	Total
GRBU01	31.74	48.48	14.89	2.16	-	1.30	-	-	-	0.03	-	1.22	0.17	100
GRBU02	24.89	52.22	18.02	2.88	-	0.50	0.08	-	0.08	-	-	1.05	0.28	100
GRBU03	16.47	48.99	24.32	9.83	-	0.04	0.18	-	0.07	0.11	-	-	-	100
GRBU04	39.26	37.26	15.33	4.50	-	1.35	0.09	-	0.03	-	-	2.06	0.12	100
GRBU05	33.18	24.89	24.45	14.27	1.03	-	0.47	0.94	0.06	0.06	-	0.22	0.44	100
GRBU06	27.33	53.91	12.17	5.74	-	0.28	-	-	-	-	-	0.58	-	100
GRBU07	30.63	54.27	10.89	0.78	-	1.14	0.08	-	0.03	-	-	2.19	-	100
GRBU08	37.13	34.78	19.89	5.09	-	-	0.11	-	0.08	0.06	0.20	1.24	1.41	100
GRBU09	28.77	51.61	12.25	5.96	-	0.06	0.22	-	0.08	0.06	-	0.72	0.28	100

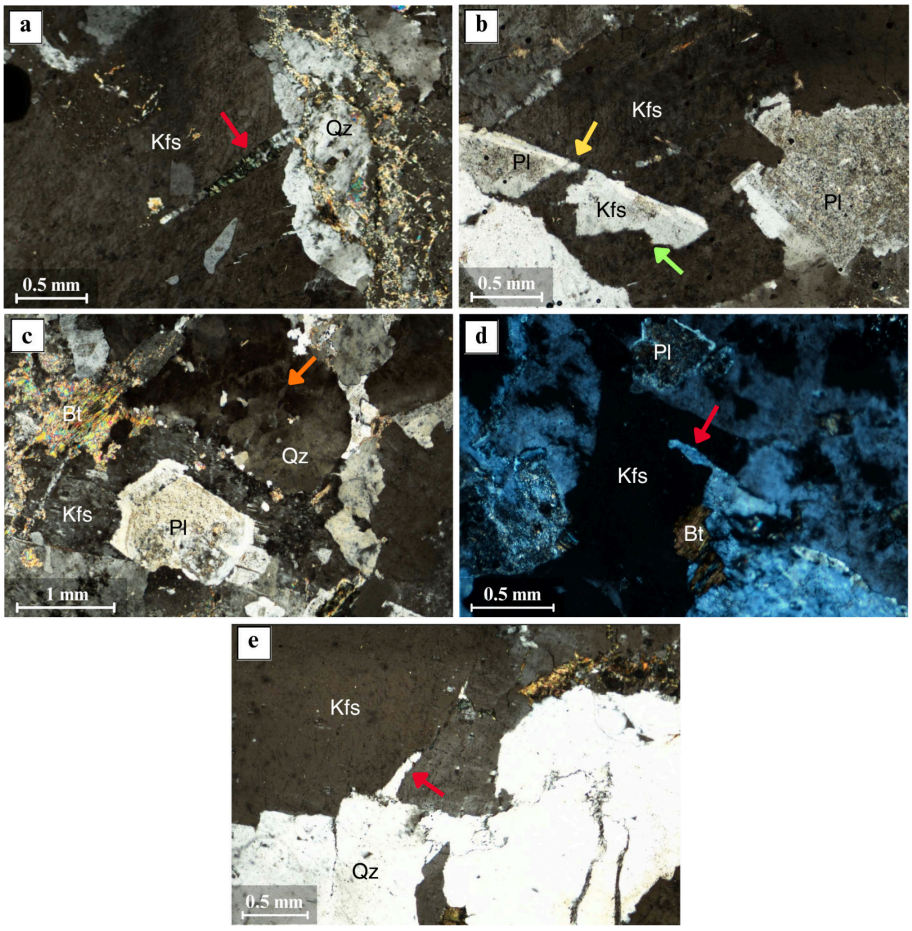


Figure 5. (**a**) Deformation in suprasolidus condition is marked by occurrence of submagmatic fractures of quartz-filled microfractures in feldspar crystals (red arrow); (**b**) grain boundary migration (GBM) showing a lobate grain boundary between plagioclase and K-feldspar (yellow arrow) and bulging recrystallization on feldspar (green arrow); (**c**) chessboard pattern extinction in quartz (orange arrow); (**d**) submagmatic fractures of quartz-filled microfractures in feldspar crystals (red arrow); (**e**) submagmatic fractures of quartz-filled microfractures in feldspar crystals (red arrow) and chessboard extinction in quartz. Mineral abbreviations: Qz = Quartz; Kfs = K-feldspar; Pl = Plagioclase; Bt = Biotite.

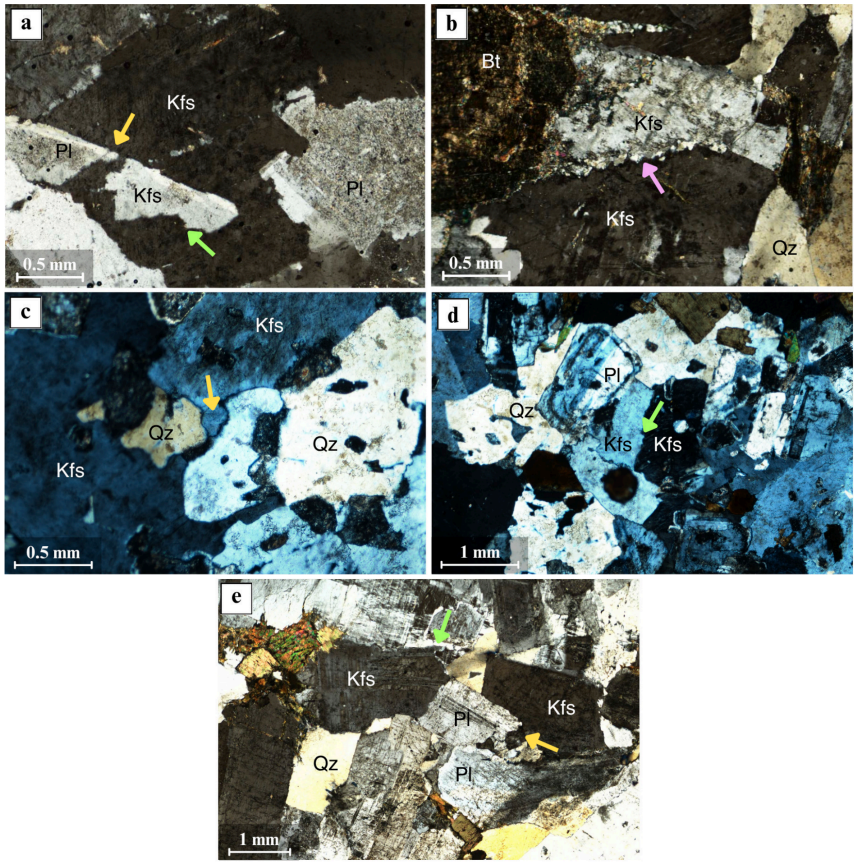


Figure 6. (**a**) Grain boundary migration (GBM) showing a lobate grain boundary between plagioclase and K-feldspar (yellow arrow) and bulging recrystallization on feldspar (green arrow); (**b**) subgrain rotation (SGR) at the boundary of K-feldspar grain (pink arrow); (**c**) plagioclase grain with normal zoning and GBM in feldspar grain (yellow arrow); (**d**) BLG in feldspar grain (green arrow); (**e**) GBM showing a lobate grain boundary (yellow arrow) and BLG in feldspar grain (green arrow). Mineral abbreviations: Qz = Quartz; Kfs = K-feldspar; Pl = Plagioclase; Bt = Biotite.

4.2.1. Microstructures Formed at Temperature Above 700 °C

The deformation microstructures formed at this temperature are associated with feldspar and quartz minerals. The microstructures of feldspar consist of submagmatic fractures and grain boundary migration (GBM) recrystallization. On the other hand, the quartz microstructure is showed by the chessboard extinction.

Submagmatic fractures on feldspar indicate late submagmatic deformation at temperature above ~700 °C [19]. This microstructure is recognized in syenogranite samples (GRBU01, GRBU04, GRBU07, and GRBU09) (Figure 5a; [19]), monzogranite samples (GRBU05 and GRBU08) (Figure 5d; [11]), and a quartz syenite sample (GRBU03) (Figure 5e; [11]). In syenogranite samples, the fractures are locally filled by quartz or fine-grained feldspathic material and are restricted to individual feldspar crystals.

The irregular and lobate boundaries of plagioclase (mainly at contact with other plagioclase grains) also imply a deformation occurred at a temperature above 700 °C, reflecting grain boundary migration (GBM) recrystallization. This microstructure can be recognized in the syenogranite samples (GRBU01, GRBU04, GRBU07, and GRBU09) (Figure 5b).

In addition, the chessboard extinction of quartz indicates a submagmatic deformation at a temperature above 700 °C. This microstructure was locally found at syenogranite samples (GRBU01, GRBU04, GRBU07, and GRBU09) (Figure 5c; [11]) and well-developed in the quartz syenite sample (GRBU03) (Figure 5e; [11]).

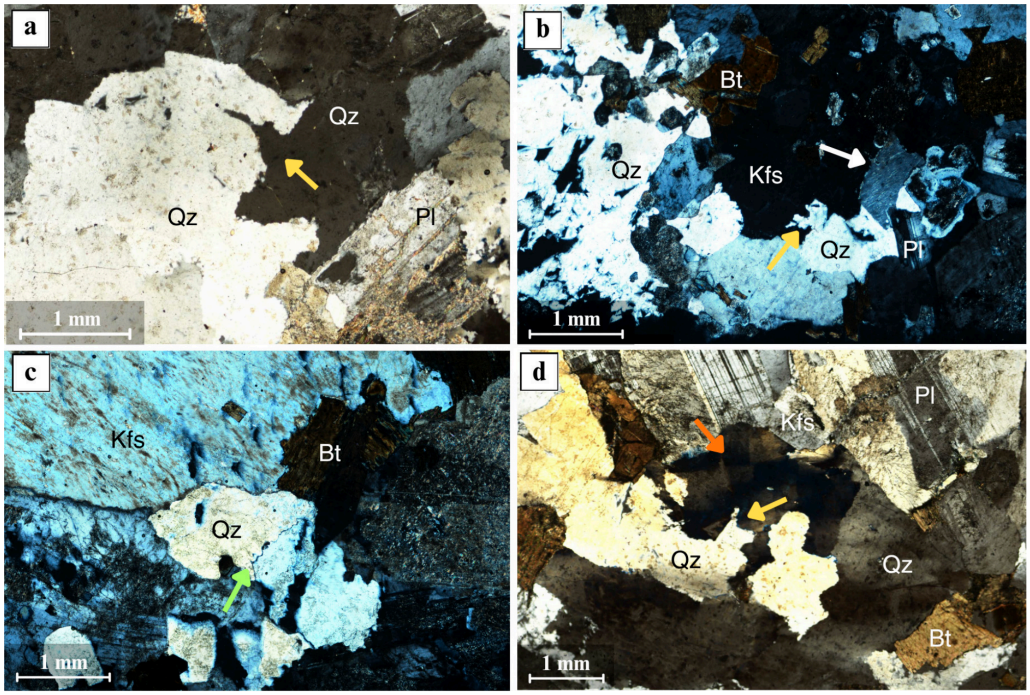


Figure 7. (**a**) GBM showing a lobate grain boundary of quartz (yellow arrow); (**b**) flame perthite (white arrow) and GBM showing a lobate grain boundary of quartz (yellow arrow); (**c**) BLG in quartz grain (green arrow); (**d**) GBM showing a lobate grain boundary of quartz (yellow arrow) and chessboard pattern quartz (orange arrow). Mineral abbreviations: Qz = Quartz; Kfs = K-feldspar; Pl = Plagioclase; Bt = Biotite.

4.2.2. Microstructure Formed at Temperature 600–700 °C

The deformation at this temperature is represented by feldspar microstructures, consisting of subgrain rotation (SGR), bulging (BLG) recrystallization, and GBM recrystallization. In syenogranite samples (GRBU01, GRBU04, GRBU07, and GRBU09), SGR and BLG recrystallization are recognized by the feldspars that show small subgrains and fine recrystallized grains along their margins, indicating a deformation temperature above 600 °C (Figure 6a,b; [11,12]). In addition, the GBM microstructure can also occur after the rock passed through the solidus temperature. Consequently, feldspar began to accommodate deformation under very high-temperature solid-state conditions (>600–700 °C) through plastic mechanisms, leading to the GBM and BLG recrystallization [11]. Figure 6c–e show the GBM and BLG recrystallization in the monzogranite (GRBU05 and GRBU08) and quartz syenite samples (GRBU03), respectively.

4.2.3. Microstructure Formed at Temperature 500–700 °C

GBM recrystallization also occurs as lobate boundaries along quartz–quartz and quartz–feldspar contacts. Because this GBM typically operates at temperatures between 500 and 700 °C [12,20,21], the high mobility of these lobate boundaries implies that deformation continued even after significant crystallization of the granitoid pluton [11,12,20]. This microstructure can be found in syenogranite samples (GRBU01, GRBU04, GRBU07, and GRBU09) (Figure 7a), monzogranite samples (GRBU05 and GRBU08) (Figure 7b,c), and quartz syenite sample (GRBU03) (Figure 7d).

4.2.4. Microstructure Formed at Temperature 450–600 °C

Myrmekite and flame perthite are the microstructures formed at this temperature. Myrmekite occurs on syenogranite, monzogranite, and quartz syenite samples, while the flame perthite only occurs on monzogranite and quartz syenite. In the syenogranite samples

(GRBU01, GRBU04, GRBU07, and GRBU09), the myrmekite intergrowths—comprising vermicular quartz within sodic plagioclase—occur along quartz–plagioclase boundaries (Figure 8a). These serve as deformation-assisted replacement or reaction textures that indicate temperatures of 450–600 °C [11]. In the monzogranite samples (GRBU05 and GRBU08) and quartz syenite sample (GRBU03), the presence of myrmekite and flame perthite indicates that the subsequent high-temperature (HT) solid-state deformation is dominated by deformation-induced reaction and exsolution textures which happen at temperature approximately ~450–600 °C [11,13,16]. Figure 8b–d show the myrmekite and flame perthite microstructures in monzogranite and quartz syenite, respectively.

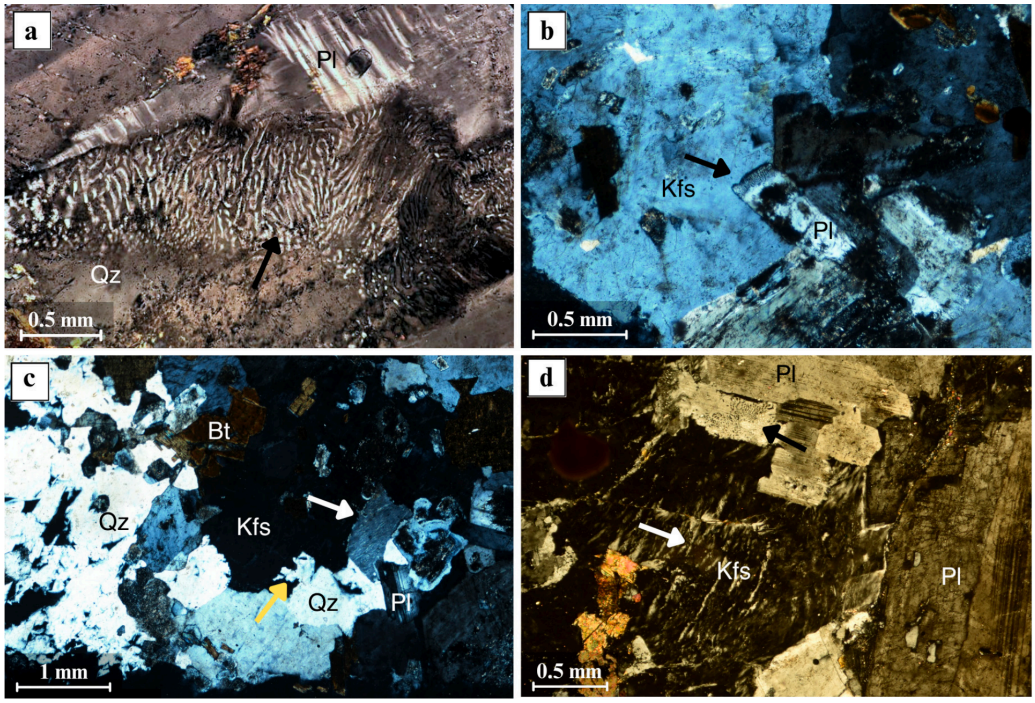


Figure 8. (**a**) Myrmekite showing intergrowth texture between plagioclase and quartz; (**b**) myrmekite showing intergrowth texture between plagioclase and quartz (black arrow); (**c**) flame perthite (white arrow) and GBM showing a lobate grain boundary of quartz (yellow arrow); (**d**) myrmekite (black arrow) and flame perthite showing intergrowth texture between K-feldspar and plagioclase (white arrow). Mineral abbreviations: Qz = Quartz; Kfs = K-feldspar; Pl = Plagioclase; Bt = Biotite.

4.2.5. Microstructure Formed at Temperature 400–500 °C

Flame perthite and SGR recrystallization are microstructures developed at this temperature. The flame perthite is locally observed in K-feldspar as irregular, flame-shaped albite lamellae (Figure 9a). These exsolution features result from solid-state deformation [13,16] and constrain deformation temperatures to 450–500 °C [11]. This microstructure is observed in syenogranite samples (GRBU01, GRBU04, GRBU07, and GRBU09).

SGR recrystallization is also developed along the margins of larger quartz grains, manifesting as subgrains and small recrystallized grains surrounding larger relict crystals. This mechanism indicates deformation at temperatures of ~400–500 °C [12,21]. This microstructure occurs on the syenogranite samples (GRBU01, GRBU04, GRBU07, and GRBU09) (Figure 9b) and quartz syenite sample (GRBU03) (Figure 9c).

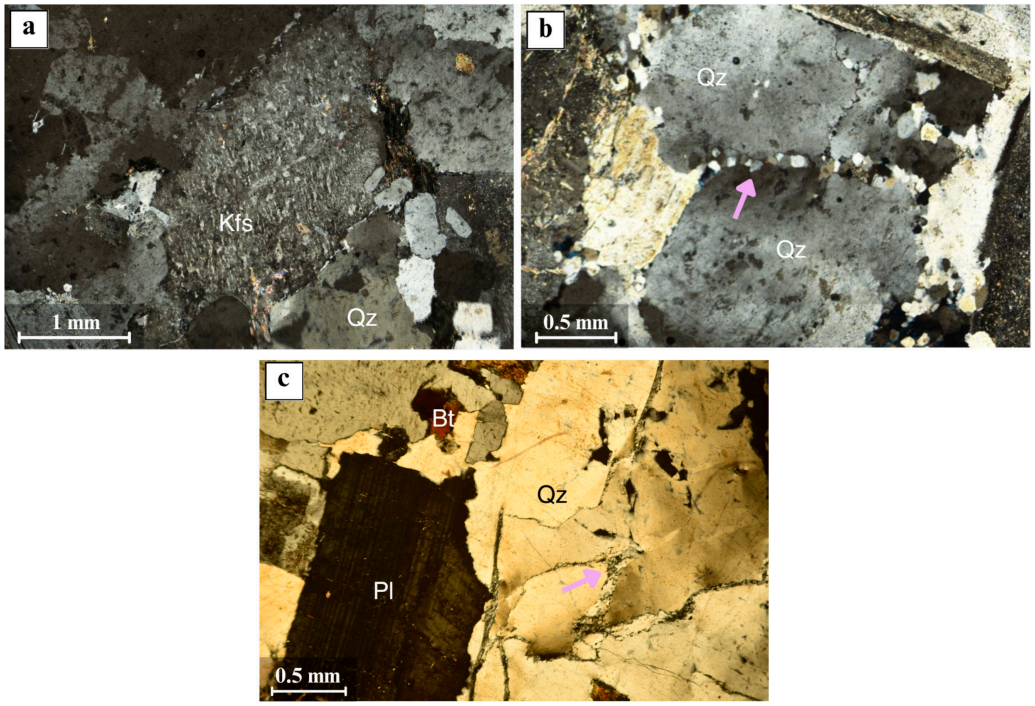


Figure 9. (**a**) Flame perthite showing intergrowth texture between K-feldspar and plagioclase; (**b**) subgrain rotation (SGR) at the boundary of quartz grain (pink arrow); (**c**) SGR (pink arrow) and undulose extinction in quartz grains. Mineral abbreviations: Qz = Quartz; Kfs = K-feldspar; Pl = Plagioclase; Bt = Biotite.

4.2.6. Microstructure Formed at Temperature 350–450 °C

In syenogranite samples (GRBU01, GRBU04, GRBU07, and GRBU09), the presence of deformed polysynthetic twins, bent twin lamellae, and localized microfracturing in plagioclase denotes the deformation temperatures below 450 °C [11], reflecting conditions under which feldspar accommodated mechanical strain more rigidly than quartz. Figure 10a shows the deformed microstructures of plagioclase in the syenogranite samples.

In monzogranite (GRBU05 and GRBU08) and quartz syenite (GRBU03) samples, the occurrence of deformed twin microstructures indicates that the feldspar responded to deformation in a more rigid manner, as temperatures continued to decrease into the low-temperature (LT) solid-state regime (~350–450 °C) [11]. Figure 10c,e show the deformed twin microstructures of feldspar in monzogranite and quartz syenite, respectively.

In addition, the undulose extinction and bulging (BLG) recrystallization microstructures represent the lower temperature deformation of quartz. The BLG recrystallization is characterized by small neoblasts along grain boundaries, typical of deformation below 400 °C [11,21]. Figure 10b,d,e show the quartz microstructures in the syenogranite (GRBU01, GRBU04, GRBU07, and GRBU09), monzogranite (GRBU05 and GRBU08), and quartz syenite (GRBU03) samples, respectively.

4.2.7. Microstructure Formed at Temperature Below 250 °C

The deformation microstructure at this temperature is associated with mica. In the syenogranite samples (GRBU01, GRBU04, GRBU07, and GRBU09), mica is represented mainly by biotite, with minor muscovite occurring locally as isolated flakes or intergrowths with biotite. Biotite commonly occurs as subhedral to anhedral flakes distributed between quartz and feldspar grains. In several samples, biotite forms small aggregates along feldspar boundaries and locally defines a weak preferred orientation at the thin-section scale. The most common deformation-related microstructures in mica are dynamic recrystallization

and kink banding, which indicate deformation temperatures above 250 °C (Figure 11a; [11]). Kink bands are observed in biotite flakes as sharp deflections of the basal cleavage, reflecting intracrystalline deformation under lower-temperature solid-state conditions. Muscovite is less abundant than biotite, but where present, it locally exhibits slight bending and cleavage distortion. Some muscovite flakes occur along feldspar boundaries, suggesting they may have formed or recrystallized during late-magmatic to subsolidus re-equilibration.

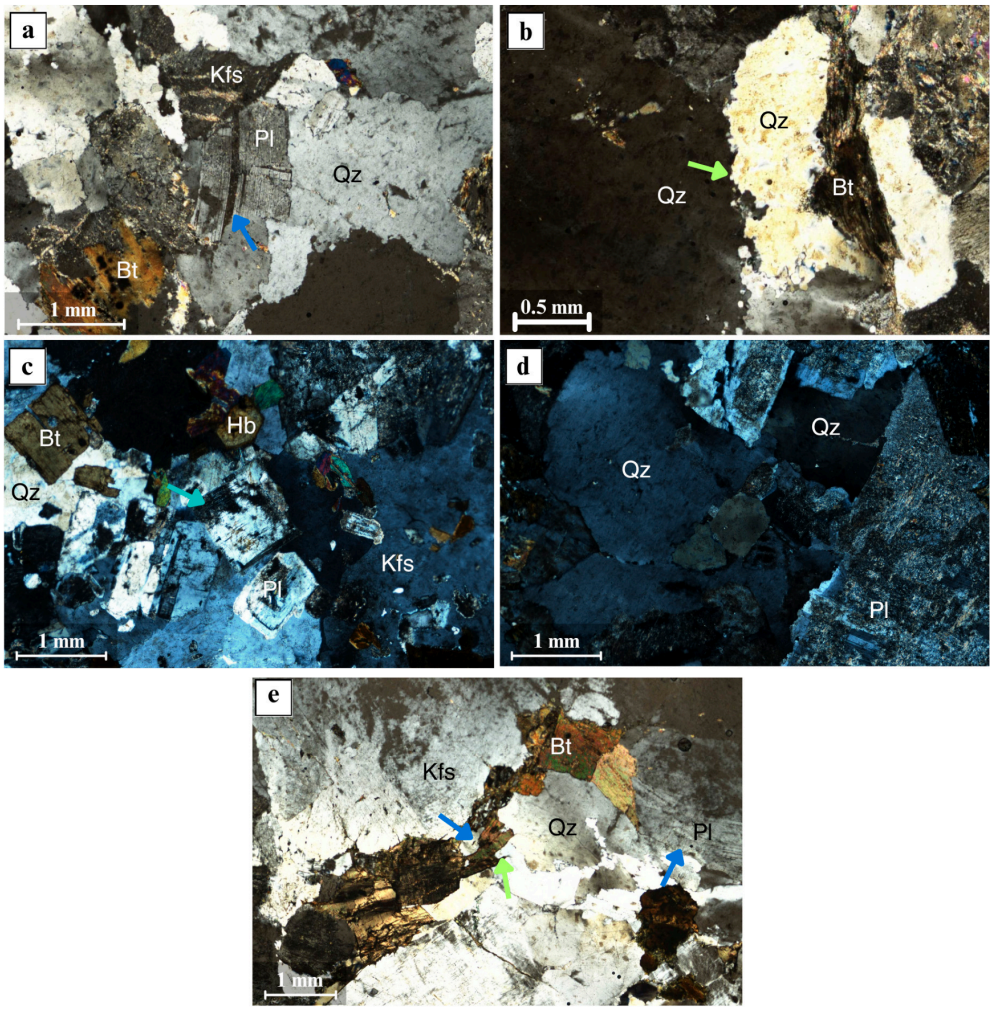


Figure 10. (**a**) Undulose extinction in quartz grain and plagioclase grain with kink bands (blue arrow); (**b**) bulging recrystallization (BLG) on quartz at the boundary of quartz grain (green arrow); (**c**) plagioclase grain with deformed twin (cyan arrow); (**d**) quartz grain with undulose extinction; (**e**) biotite and plagioclase grain with kink bands (blue arrow) and quartz showing BLG recrystallization (green arrow). Mineral abbreviations: Qz = Quartz; Kfs = K-feldspar; Pl = Plagioclase; Bt = Biotite; Hb = Hornblende.

In monzogranite samples (GRBU05 and GRBU08), mica is represented by biotite. The kink bands of biotite also exist which indicate intracrystalline plastic deformation before brittle fracturing occurred at lower temperatures below 250 °C (Figure 11b; [11,20]).

Mica in the quartz syenite sample (GRBU03) is represented mainly by biotite, with minor muscovite occurring locally as isolated flakes or intergrowths with biotite. Kink bands also occur which indicate intracrystalline plastic deformation before brittle fracturing occurred at lower temperatures below 250 °C (Figure 11b; [11,20]).

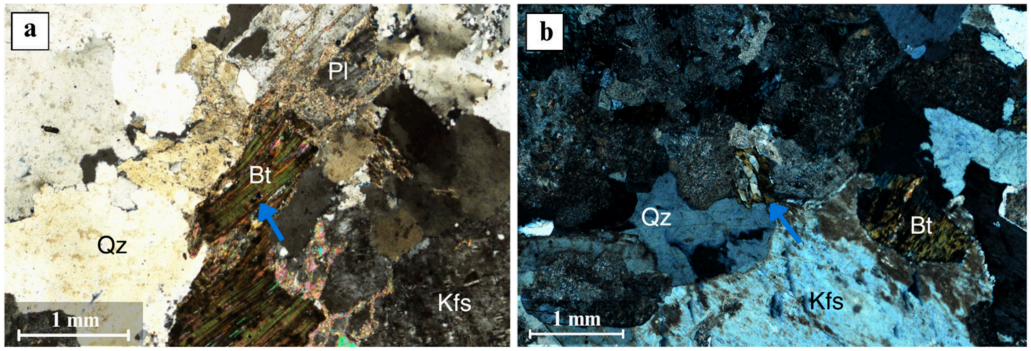


Figure 11. (**a**) Biotite grain with kink bands (blue arrow); (**b**) biotite grain with kink bands (blue arrow). Mineral abbreviations: Qz = Quartz; Kfs = K-feldspar; Pl = Plagioclase; Bt = Biotite.

5. Discussion

5.1. Microstructural Evolution of North Bangka Granitoids

The microstructural record of North Bangka granitoids documents a continuous deformation history spanning from the suprasolidus (T > 650 °C) through the high-temperature subsolidus (650–450 °C) to the low-temperature subsolidus regime (T < 450 °C), as summarized in Figure 12 and Table 4.

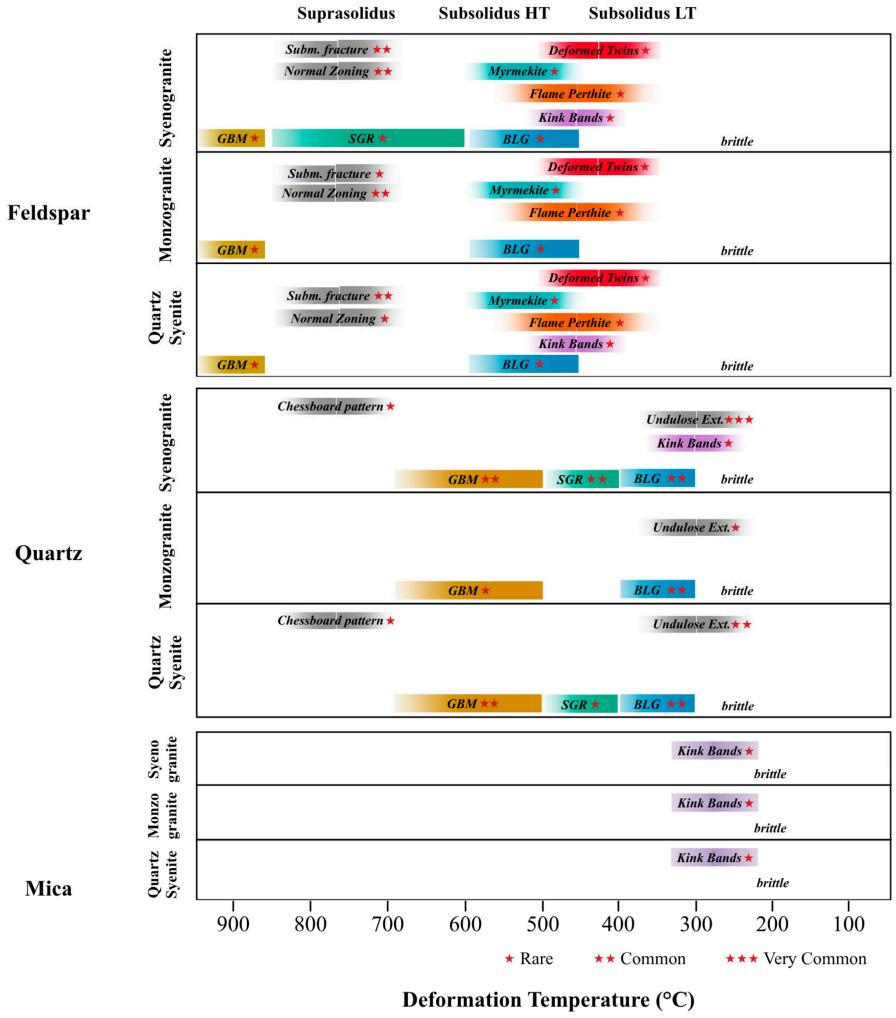


Figure 12. Temperature–deformation stage diagram for North Bangka granitoids, showing the temperature ranges of diagnostic microstructures. Temperature estimates based on [11–13].

Table 4. Summary of diagnostic microstructures, formation conditions, and geological interpretation.

Diagnostic Microstructure	Formation Condition	Geological Interpretation
STAGE 1: Suprasolidus (T > 650 °C)		
Submagmatic fractures	T > 650 °C; melt still present; crystallization incomplete	Fractures formed at late magmatic stage during build-up of crystallization pressure
GBM in feldspar (lobate grain boundaries)	High-T grain boundary mobility in the presence of residual melt	High-T GBM recrystallization producing lobate boundaries; indicates magmatic or near-solidus deformation
Normal zoning in plagioclase	Magma crystallization still active	Primary magmatic texture reflecting compositional evolution during fractional crystallization
Chessboard extinction in quartz	T > 550 °C; combined basal and prism slip activated	Indicates deformation at high temperature during late-stage crystallization
STAGE 2: Subsolidus HT (650 °C > T > 450 °C)		
GBM recrystallization in quartz	Fully solid state; T still high; mobile grain boundaries	Grain coarsening by boundary migration; lobate quartz–quartz contacts
Subgrain rotation (SGR)	Solid state; dislocation accumulation and rotation	Progressive misorientation of subgrains into new grains; intermediate T regime
Myrmekite	K-feldspar reacting with Na-rich fluid or melt	Replacement of K-feldspar margin by vermicular Qz + Ab; driven by Na metasomatism during deformation
Flame perthite	Solid-state replacement of K-feldspar by albite	Diffusion-controlled exsolution or replacement under deformation; indicates T < solidus
STAGE 3: Subsolidus LT (T < 450 °C)		
Undulose extinction; BLG	T < 400–450 °C; dislocation creep and BLG dominant	Fine neoblasts along old grain boundaries; lowest-T recrystallization mechanism
Deformation twins; kink bands	Mechanical deformation of feldspar/plagioclase and mica	Crystal-plastic deformation at low T; records the latest stress episode

5.1.1. Stage 1—Suprasolidus Deformation (T > 650 °C)

The presence of submagmatic fractures provides unequivocal evidence that deformation initiated while a residual melt phase was still present within the crystallizing magma body [19]. These fractures are partially healed by quartz and feldspar, consistent with crack-sealing by late melt films or hydrothermal fluids. GBM in feldspar and normal plagioclase zoning confirm that crystallization was ongoing during the early stages of deformation, corroborating a syn-magmatic deformation component [17]. The presence of chessboard extinction in quartz indicates temperatures above 550 °C, where both basal <a> and prism [c] slip systems are activated simultaneously [11].

5.1.2. Stage 2—High-Temperature Subsolidus Deformation (650–450 °C)

Following complete solidification, deformation continued at elevated temperatures in the fully solid state. GBM recrystallization in quartz, characterized by highly lobate and sutured grain boundaries, is the dominant mechanism at this stage, consistent with

temperatures of 500–700 °C [12]. Coeval SGR recrystallization in quartz, producing new grains from progressively misoriented subgrains, indicates the transition toward a lower-temperature GBM regime. Myrmekite formation along K-feldspar boundaries in contact with plagioclase is interpreted as a stress-driven reaction involving influx of Na-rich fluids and local volume reduction [9]. Flame perthite documents the diffusion-controlled replacement of K-feldspar by albite under deformation conditions [16]. It should be noted that the temperature boundaries of the deformation stages are primarily constrained by feldspar and melt-present microstructures (e.g., submagmatic fractures, grain-boundary migration in feldspar, myrmekite, and flame perthite). Quartz recrystallization fabrics (GBM, SGR, and BLG) can persist across these stage boundaries and are therefore used as supporting, rather than strictly delimiting, indicators. Consequently, the assignment of SGR (typically calibrated at ~400–500 °C) within the broader 650–450 °C stage does not represent a contradiction between the two thermometric frameworks.

5.1.3. Stage 3—Low-Temperature Subsolidus Deformation (T < 450 °C)

The final stage of deformation is marked by microstructures diagnostic of lower-temperature crystal plasticity and mechanical deformation. Undulose extinction and BLG in quartz indicate dislocation creep and grain boundary area reduction under low-temperature conditions (<400 °C) [12]. Deformation twins in plagioclase and kink bands in biotite and muscovite reflect mechanical deformation in the crystal-plastic to frictional transition regime. The systematic development of these features across all lithological types confirms that deformation was pervasive and persisted well into the solid state as the pluton cooled to ambient crustal temperatures.

5.2. Tectonic Implications

The continuous microstructural record from suprasolidus to low-temperature subsolidus conditions implies that the North Bangka granitoids experienced syn- to post-magmatic deformation driven by a persistent regional tectonic stress field (Table 4).

A critical question is whether the observed deformation record reflects a single protracted syn- to post-magmatic event or a later, purely post-magmatic tectonic overprint (e.g., Jurassic–Cretaceous reactivation of regional structures). The microstructural evidence strongly supports the former interpretation and effectively rules out a discrete later overprint. Submagmatic fractures in feldspar, which form only in the presence of residual melt at temperatures > 650–700 °C [19], provide unequivocal evidence that deformation was already active while the magma was still crystallizing. Similarly, chessboard extinction in quartz and grain boundary migration (GBM) in feldspar require high-temperature conditions that could only exist shortly after emplacement. A purely post-magmatic reactivation during the Jurassic–Cretaceous would have occurred long after the Klabat Granite (crystallization ages 219–227 Ma) had cooled to ambient crustal temperatures, and thus could only produce low-temperature or brittle deformation features.

Furthermore, the continuous and progressive sequence from suprasolidus (submagmatic fractures, GBM in feldspar, chessboard quartz, normal plagioclase zoning) through high-temperature subsolidus (myrmekite, flame perthite, GBM/SGR in quartz) to low-temperature subsolidus microstructures (BLG, undulose extinction, deformation twins, kink bands) without any thermal hiatus or overprinting textures indicates a single, protracted deformation history. This interpretation is consistent with published criteria for distinguishing syn-magmatic from post-magmatic deformation in granitoids [17,19].

The initiation of deformation at suprasolidus conditions (Stage 1) demonstrates that tectonic stress was already active during the emplacement and crystallization of the Klabat Granite. This is consistent with the Late Triassic Sibumasu–Indochina collision [6], which created the regional NNW–SSE and NNE–SSW structural framework documented in North Bangka [5]. Syn-magmatic deformation of granite intrusions has been documented in analogous settings within the SATB [22] and in other Hercynian and Alpine plutons [23].

The persistence of deformation from suprasolidus through low-temperature subsolidus conditions indicates that the regional stress field remained active during and immediately after emplacement and cooling of the Klabat Granite. This protracted history is best explained by prolonged post-collisional deformation following the Late Triassic Sibumasu–Indochina collision [6], which established the regional NNW–SSE and NNE–SSW structural framework in North Bangka [5]. Although later tectonic reactivation during Jurassic–Cretaceous oblique subduction along the Sunda margin [7] may have occurred, it cannot account for the high-temperature microstructural record (e.g., submagmatic fractures, chessboard quartz, myrmekite, and flame perthite) preserved in the granitoids. The absence of a ductile foliation at the hand-specimen scale, combined with evidence of distributed crystal-plastic deformation, further suggests that strain was accommodated under pluton-wide stress rather than being localized within discrete shear zones.

Comparison with the published microstructural record of granitoids from Peninsular Malaysia and Belitung [8,22] reveals similar temperature–deformation sequences, supporting a common tectono-magmatic heritage across the SATB. The microstructural data presented here thus provide a new constraint on the timing and mechanism of deformation in the Indonesian sector of the belt. The integrated tectono-microstructural evolution of the North Bangka granitoids is summarized schematically in Figure 13, illustrating the transition from syn-magmatic emplacement to progressive post-magmatic solid-state deformation under continued regional compression.

5.2.1. Implications for Granite Emplacement in the SATB

The occurrence of submagmatic fractures, feldspar grain-boundary migration (GBM), and chessboard quartz suggests that deformation initiated before complete crystallization of the granitoid magma. These microstructures indicate that the North Bangka granitoids were emplaced under an active stress regime rather than under tectonically quiescent conditions. Similar relationships between granite emplacement and deformation have been documented in granitoid provinces throughout the Southeast Asian Tin Belt (SATB), where magmatism is commonly interpreted as being linked to subduction, continental collision, and post-collisional tectonic processes [2,8,11,24,25]. The Late Triassic granitoids of the Main Range Province in Peninsular Malaysia, for example, have been interpreted as syn- to post-collisional granitoids generated during closure of the Paleo-Tethys Ocean and collision between the Sibumasu and Indochina terranes [8]. Consequently, the deformation record preserved in the North Bangka granitoids may reflect a broader tectono-magmatic framework in which magma emplacement and regional deformation were closely coupled during the final stages of SATB evolution.

5.2.2. Regional Comparison with Other SATB Granitoids

The microstructural evolution documented in the North Bangka granitoids is broadly comparable to deformation histories reported from granitoids elsewhere in the SATB. Previous studies have shown that many granitoid bodies within the Main Range Province of Peninsular Malaysia and adjacent regions experienced prolonged tectono-magmatic evolution involving magma emplacement, crystallization, and subsequent solid-state deformation [8,25]. Such granitoids commonly record evidence for syn-magmatic deformation

followed by progressive high-temperature and low-temperature subsolidus overprinting. Although the intensity and duration of deformation vary among individual plutons, the overall progression from magmatic to solid-state deformation appears to be a recurring characteristic of SATB granitoids. This similarity suggests that deformation was not restricted to individual intrusions but instead reflects regional-scale tectonic processes associated with Paleo-Tethyan closure, terrane amalgamation, and post-collisional crustal reorganization across Southeast Asia [8]. The North Bangka granitoids therefore provide additional microstructural evidence for prolonged tectono-magmatic interaction within the Indonesian segment of the SATB.

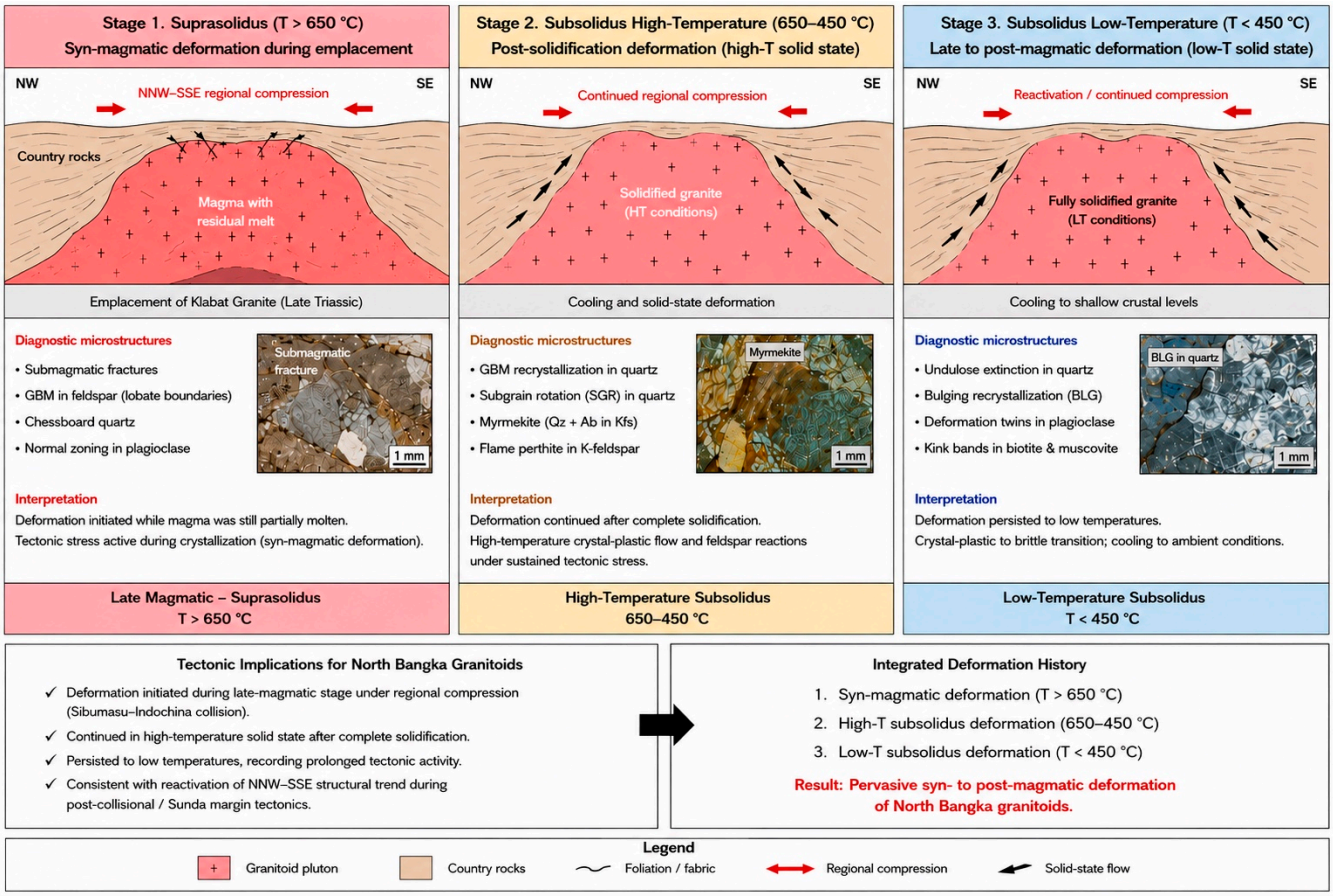


Figure 13. Schematic tectonic model illustrating the progressive deformation evolution of the North Bangka granitoids from syn-magmatic emplacement to post-magmatic solid-state deformation (not to scale). Stage 1 (suprasolidus; T > 650 °C) records syn-magmatic deformation during emplacement of the Klabat Granite under regional compression, characterized by submagmatic fractures, feldspar grain-boundary migration (GBM), chessboard quartz, and normal plagioclase zoning. Stage 2 (high-temperature subsolidus; 650–450 °C) represents continued deformation after complete solidification, marked by quartz GBM and subgrain rotation (SGR) recrystallization, myrmekite development, and flame perthite formation. Stage 3 (low-temperature subsolidus; T < 450 °C) reflects persistent deformation during cooling to shallow crustal conditions, evidenced by undulose extinction, bulging recrystallization (BLG), deformation twins, and kink bands in mica. The integrated model is consistent with deformation occurring during or after the tectonic processes associated with the Sibumasu–Indochina collision. Regional compression explained by red arrow and solid-state flow explained by black arrow.

6. Conclusions

This study documents a continuous record of deformation in the North Bangka granitoids, spanning from suprasolidus magmatic conditions to low-temperature solid-state deformation. The microstructural assemblage demonstrates that deformation began during the final stages of magma crystallization and continued throughout pluton cooling. These observations indicate that granitoid emplacement occurred within an active tectonic regime and was followed by prolonged regional deformation. Comparison with other granitoids from the Southeast Asian Tin Belt suggests that such syn- to post-magmatic deformation may represent a common feature of granitoid evolution across the belt. Consequently, the North Bangka granitoids provide important microstructural constraints on the tectono-magmatic evolution of the Indonesian segment of the Southeast Asian Tin Belt.

Author Contributions: Conceptualization, M.I.S., M.A. and N.I.B.; methodology, M.I.S. and M.A.; formal analysis, M.I.S.; investigation, M.I.S.; data curation, M.I.S.; writing—original draft preparation, M.I.S., M.A., N.I.B., E.S., I.G.B.E.S., P.S., M.F.R.Y. and M.B.N.; writing—review and editing, M.I.S., M.A., N.I.B., and M.F.R.Y.; supervision, M.A. and N.I.B. All authors have read and agreed to the published version of the manuscript.

Funding: This research received no specific external funding. The research was conducted as part of the graduate research program at the Department of Geological Engineering, Institut Teknologi Bandung (ITB).

Data Availability Statement: The data supporting the findings of this study are available from the corresponding author upon reasonable request.

Acknowledgments: The authors gratefully acknowledge Slamet Sugiharto and PT Timah Indonesia for kindly providing and facilitating access to the granite samples from North Bangka. We are also indebted to our colleagues and the academic staff at Institut Teknologi Bandung (ITB) for their valuable discussions and suggestions, which significantly improved the petrographic and microstructural interpretations in this study.

Conflicts of Interest: The authors declare no conflicts of interest.

Abbreviations

Ap	Apatite
BLG	Bulging Recrystallization
Bt	Biotite
Chl	Chlorite
GBM	Grain Boundary Migration
Hb	Hornblende
Kfs	K-Feldspar
Ms	Muscovite
Opq	Opaque Mineral
Pl	Plagioclase
Px	Pyroxene
Qz	Quartz
SATB	Southeast Asian Tin Belt
Ser	Sericite
SGR	Subgrain Rotation
Tur	Tourmaline
Xen	Xenolith
Zrn	Zircon

References

1. Cobbing, E.J.; Mallick, D.I.J.; Pitfield, P.E.J.; Teoh, L.H. The granites of the Southeast Asian Tin Belt. *J. Geol. Soc.* **1986**, *143*, 537–550. [CrossRef]
2. Schwartz, M.O.; Rajah, S.S.; Askury, A.K.; Putthapiban, P.; Djaswadi, S. The Southeast Asian Tin Belt. *Earth-Sci. Rev.* **1995**, *38*, 95–293. [CrossRef]
3. Katili, J.A. Structure and age of the Indonesian tin belt with special reference to Bangka. *Tectonophysics* **1967**, *4*, 403–418. [CrossRef]
4. Ko, U.K. Preliminary synthesis of the geology of Bangka Island, Indonesia. *Geol. Soc. Malays. Bull.* **1986**, *20*, 81–96. [CrossRef]
5. Mangga, S.A.; Djamal, B. *Peta Geologi Lembar Bangka Utara, Sumatera*; Pusat Penelitian dan Pengembangan Geologi: Bandung, Indonesia, 1994.
6. Metcalfe, I. Gondwana dispersion and Asian accretion: Tectonic and palaeogeographic evolution of eastern Tethys. *J. Asian Earth Sci.* **2013**, *66*, 1–33. [CrossRef]
7. Hall, R. The plate tectonics of Cenozoic SE Asia and the distribution of land and sea. In *Biogeography and Geological Evolution of SE Asia*; Backhuys Publishers: Leiden, The Netherlands, 1998; pp. 99–131.
8. Ng, S.W.-P.; Whitehouse, M.J.; Roselee, M.H.; Teschner, C.; Murtadha, S.; Oliver, G.J.; Ghani, A.A.; Chang, S.-C. Late Triassic granites from Bangka, Indonesia: A continuation of the Main Range granite province of the South-East Asian Tin Belt. *J. Asian Earth Sci.* **2017**, *138*, 548–561. [CrossRef]
9. Nedelec, A.; Bouchez, J.L. *Granites: Petrology, Structure, Geological Setting, and Metallogeny*; Oxford University Press: New York, NY, USA, 2015.
10. Vernon, R.H. Granites Really Are Magmatic: Using Microstructural Evidence to Refute Some Obstinate Hypotheses. *J. Virtual Explor.* **2010**, *35*, 1–36. [CrossRef]
11. Passchier, C.W.; Trouw, R.A.J. *Microtectonics*; Springer: Berlin/Heidelberg, Germany, 2005. [CrossRef]
12. Stipp, M.; Stünitz, H.; Heilbronner, R.; Schmid, S.M. The eastern Tonale fault zone: A 'natural laboratory' for crystal plastic deformation of quartz over a temperature range from 250 to 700 °C. *J. Struct. Geol.* **2002**, *24*, 1861–1884. [CrossRef]
13. Vernon, R.H. *A Practical Guide to Rock Microstructure*; Cambridge University Press: Cambridge, UK, 2018. [CrossRef]
14. Gill, R. *Igneous Rocks and Processes: A Practical Guide*; Wiley-Blackwell: Oxford, UK, 2010.
15. Streckeisen, A. Classification and nomenclature of plutonic rocks: Recommendations of the IUGS subcommission on the systematics of igneous rocks. *Geol. Rundsch.* **1974**, *63*, 773–786. [CrossRef]
16. Pryer, L.L.; Robin, P.-Y.F. Retrograde metamorphic reactions in deforming granites and the origin of flame perthite. *J. Metamorph. Geol.* **1995**, *13*, 645–658. [CrossRef]
17. Paterson, S.R.; Vernon, R.H.; Tobisch, O.T. A review of criteria for the identification of magmatic and tectonic foliations in granitoids. *J. Struct. Geol.* **1989**, *11*, 349–363. [CrossRef]
18. Whitney, D.L.; Evans, B.W. Abbreviations for Names of Rock-Forming Minerals. *Am. Mineral.* **2010**, *95*, 185–187. [CrossRef]
19. Bouchez, J.L.; Delas, C.; Gleizes, G.; Nedelec, A.; Cuney, M. Submagmatic microfractures in granites. *Geology* **1992**, *20*, 35–38. [CrossRef]
20. Russo, D.; Fiannacca, P.; Fazio, E.; Cirrincione, R.; Mamtani, M.A. Geology and microstructural evolution of syn- to late-tectonic granitoids from Capo Vaticano Promontory (southern Calabria, Italy). *Geol. Mag.* **2024**, *162*, e8. [CrossRef]
21. Law, R.D. Deformation thermometry based on quartz c-axis fabrics and recrystallization microstructures: A review. *J. Struct. Geol.* **2014**, *66*, 129–161. [CrossRef]
22. Barbarin, B. A review of the relationships between granitoid types, their origins and their geodynamic environments. *Lithos* **1999**, *46*, 605–626. [CrossRef]
23. Aurejac, J.-B.; Gleizes, G.; Diot, H.; Bouchez, J.-L. Le complexe granitique de Querigut (Pyrenees, France) réexaminé par la technique de l'ASM: Un pluton syntectonique de la transpression dextre hercynienne. *Bull. Soc. Géol. Fr.* **2004**, *175*, 660–661. [CrossRef]
24. Mitchell, A.H.G. Tectonic Settings for Emplacement of Southeast Asian Tin Granites. *Bull. Geol. Soc. Malays.* **1977**, *9*, 123–140. [CrossRef]
25. Krähenbühl, R. Magmatism, Tin Mineralization and Tectonic Development of the Main Range, Malaysian Peninsula: Consequences for the Plate Tectonic Model of Southeast Asia Based on Rb-Sr, K-Ar and Fission Track Data. *Bull. Geol. Soc. Malays.* **1991**, *29*, 1–100. [CrossRef]

Disclaimer/Publisher's Note: The statements, opinions and data contained in all publications are solely those of the individual author(s) and contributor(s) and not of MDPI and/or the editor(s). MDPI and/or the editor(s) disclaim responsibility for any injury to people or property resulting from any ideas, methods, instructions or products referred to in the content.